

The Adaptive Tobit Kalman Filter: Tracking Position with Censored Measurements in the IoT

Federico Chiariotti

Department of Information Engineering, University of Padova
Via Gradenigo, 6/b, 35131 Padova, Italy. Email: chiariot@dei.unipd.it

Abstract—In the Internet of Things (IoT) paradigm, distributed sensors and actuators can observe and act on their environment, communicating wirelessly. In this context, filtering the observations and tracking the network and environment state over time is extremely important, and the Kalman Filter (KF) is one of the most common tools for this. Several of these applications deal with censored data, either because of sensor saturation or limited detection regions: when censoring happens, all measurements below a certain threshold are clipped to the threshold value. The recently proposed Tobit Kalman Filter (TKF) is an adjusted version of the KF that can deal with censored measurements. However, like the traditional KF, it needs full knowledge of the process and measurement noise covariances to work, which are not always available in practice. In this work, we relax this assumption and propose the Adaptive Tobit Kalman Filter (ATKF), which can dynamically estimate the process and measurement noise along with the hidden state of the system from the censored measurements. We apply our solution to navigation and positioning IoT scenarios, obtaining a negligible performance loss with regard to the TKF, even with no *a priori* knowledge of the noise statistics.

I. INTRODUCTION

The Internet of Things (IoT) is a paradigm that exploits ubiquitous sensing by a myriad of low-power connected devices [1]. Several IoT services aggregate sensor measurements and track important variables, such as the location of users and nodes [2], over time. Filtering tools and estimators are commonly deployed in order to perform sensor data fusion [3] and correct for sensor error and drift [4].

Localization and motion tracking are key aspects of the IoT [5]: several services need to be aware of users' and nodes' location to improve performance [6], or even to work at all [7]. The development of accurate filtering and tracking tools to predict the future position from past measurements [8] can significantly improve these services' performance by introducing anticipatory elements [9] in the optimization.

The Kalman Filter (KF) [10] is the optimal estimator for linear dynamic systems, and it is now used in a wide range of IoT positioning and tracking applications, based on wireless signals [11], video object recognition [12] and vehicle GPS [13]. The KF exploits knowledge of the system model to estimate a hidden state from noisy measurements. However, its performance degrades strongly when there are nonlinearities in the system or non-Gaussian noise distributions. One of the most common nonlinearities is Tobit Type I censoring [14]: in this kind of model, measurements have a saturation threshold (that might be due to sensor saturation, detection limits, or

occlusion), and any value below the threshold is clipped. It is easy to extend the model to the case with an upper threshold instead of a lower one, or even to the doubly censored case. The Tobit Kalman Filter (TKF) [15] is a recent adaptation of the standard KF that can deal with this kind of nonlinearities.

However, an important assumption of the KF is the full knowledge of the noise statistics: in order to correctly separate changes in the hidden state from measurement noise, the filter needs the covariance matrices of the process and measurement noise.

Leveraging the approaches proposed in [15] and [16], this work derives the Adaptive Tobit Kalman Filter (ATKF): this filter can overcome both the censoring issue and the noise estimation problem, correctly estimating the state with no *a priori* knowledge of the noise covariance even when most of the measurements are censored. First, the unbiased noise estimator from [16] is adapted to obtain the one-step Maximum Likelihood Estimator (MLE) for the Tobit case. The ATKF is then tested in a simple scenario and two real IoT navigation and networking applications, showing that its performance is close to the full-knowledge TKF's.

The rest of this paper is organized as follows: in Sec. III, the Tobit model and standard TKF are presented. In Sec. IV, the ATKF is derived using the noise estimator in [16]. The simulation results are shown in Sec. V, and Sec. VI concludes the paper and lists some possible avenues of future work.

II. RELATED WORK

Kalman filtering is one of the most used tools in IoT tracking applications, with examples in very different domain. Smart Grid management can be helped by the use of KFs to track the voltage in a microgrid remotely even with noisy communication channels [17], and in [18], a KF is used to predict the amount of energy that the wireless nodes will harvest in the near future, guiding routing decisions. It can even be used to track traffic jams [19] or health-related cycling metrics and statistics [20]. Kalman filtering can also aid distributed sensing, to improve the accuracy of the tracked variable or to reduce useless communications [21] by tracking the channel and the usefulness of the transmission.

Localization and ranging are two of the applications in which KFs are used most often: while several methods to gauge the position and distance of a node from radio transmissions exist, from time of arrival estimation to Received Signal Strength (RSS)-based ranging, they are often inaccurate

in complex propagation environments. KFs have been used to reduce the noise and improve the estimate accuracy using Bluetooth Low Energy (BLE) [22] and Long Range Wide Area Network (LoRaWAN) [23] signals, and a node equipped with multiple wireless interfaces can use a KF for sensor fusion to improve the overall positioning accuracy. The use of Visible Light Communication (VLC) signals in localization has recently given some good results, using KFs to reduce the measurement error [24].

The KF is a powerful tool, but its linearity requirement is restrictive; several approaches have been tried to deal with nonlinearities in the system and noise. The first approach to the Tobit censoring issue was to consider censored measurements as missing, and adapt the KF to deal with intermittent measurements [25]. However, the performance degrades significantly when the state of the system is close to the censoring region and the censoring probability is high. The TKF [15] is a recently developed tool that can achieve good performance in Type I censored systems. It calculates the expected value of the measurements after taking the censoring probability into account and uses it to find a modified innovation value. The filter assumes that the state error is small to get a recursive formulation: the diagonality of the noise covariance matrices is assumed to simplify the notation, but not strictly required. The TKF has been shown to outperform even nonlinear filters such as the Extended Kalman Filter (EKF) and Unscented Kalman Filter (UKF), with better estimates of the state uncertainty and smoother transitions from censoring to non-censoring [26]. A similar adaptation has been proposed for particle filters [27], another common filtering tool. Another work [28] uses a modified TKF to adapt to changes in the doubly censored case.

Another well-known issue of the traditional KF is its requirement of full *a priori* knowledge of the measurement and process noise covariances: in many applications, these covariances are hard to estimate in advance or even time-varying, and the design of an efficient Adaptive Kalman Filter (AKF) has been the subject of considerable research interest over the years, from the first works in the 1970s [29] to more recent approaches. The Autocovariance Least Squares (ALS) method [30] uses the autocovariance of the innovation signal to estimate the noise covariance matrices. It works in the general case of non-diagonal covariance matrices, and results in the optimal estimate, but it requires convergence of the Kalman gain before it can operate. As such, it is poorly equipped to deal with time-varying noise statistics or complex scenarios. The time-varying noise issue was solved by the unbiased one-step estimator in [16]: while not fully exploiting the historical information, this estimator can react to shifts in the noise and deal with an unstable Kalman gain. Another recent work [31] develops an Auto Regressive Integrated Moving Average (ARIMA) approach to the estimation of the process noise covariance with fast convergence when the measurement noise statistics are known.

The case of Tobit Kalman filtering with unknown parameters has been covered by a few recent works, investigating different aspects of the issue. A modified TKF presented in [32] can also deal with non-Gaussian Lévy and time-correlated

measurement noise. In this case, the noise is transformed into a Gaussian noise with unknown variance, which is estimated by a recursive process, using the *a priori* knowledge of the process noise covariance and the measurement noise time correlation. Finally, the case of uncertainty in the system model is examined in [33]: the authors introduce some randomness in the dynamic system, using stochastic update and measurement matrices with known statistics and known noise covariance matrices.

III. THE TOBIT KALMAN FILTER

We consider a dynamic linear system with Tobit Type I censoring:

$$\mathbf{x}_{k+1} = \mathbf{A}_k \mathbf{x}_k + \mathbf{w}_k \quad (1)$$

$$\mathbf{y}_k^* = \mathbf{C}_k \mathbf{x}_k + \mathbf{v}_k \quad (2)$$

$$\mathbf{y}_k = \max(\boldsymbol{\tau}_k, \mathbf{y}_k^*) \quad , \quad (3)$$

where $\mathbf{x}_k \in \mathbb{R}^n$ is a hidden state vector, $\mathbf{y}_k \in \mathbb{R}^m$ is the measurement output vector, $\mathbf{A}_k \in \mathbb{R}^{n \times n}$ is the non-singular update matrix and $\mathbf{C}_k \in \mathbb{R}^{m \times n}$ is the measurement matrix. The two components \mathbf{w}_k and \mathbf{v}_k are multivariate Gaussian random vectors with zero mean and covariance matrices $\mathbf{Q}_k \in \mathbb{R}^{n \times n}$ and $\mathbf{R}_k \in \mathbb{R}^{m \times m}$, respectively. The standard KF is the optimal estimator of the hidden state as long as there is no censoring, but the Tobit nonlinearity makes it suboptimal if some measurements are censored.

We now introduce the notation used in the following: given a random variable X , its expected value is denoted by $\mathbb{E}[X]$ and its variance is $\text{Var}[X]$. The conditional expectation of X given the value of Y is denoted by $\mathbb{E}[X|Y]$. Vectors like \mathbf{x} are written in bold, while matrices like \mathbf{A} are written in bold and indicated with capital letters. The hat symbol indicates that the value is an estimate: \hat{x} is an estimate of x . We refer to the univariate normal Probability Density Function (PDF) as $\phi(\cdot)$, and to the normal Cumulative Distribution Function (CDF) as $\Phi(\cdot)$. To simplify the notation in the following steps, we also define the elements of the vector $\boldsymbol{\eta}_k$ as:

$$\eta_k(i) = \frac{C_k \hat{x}_{k|k-1}(i) - \tau_k(i)}{\sigma_k(i)} \quad (4)$$

We also define the inverse Mills ratio, i.e., $\mathbb{E}[X|X > \alpha]$, which we denote by $\lambda(\alpha)$ for the univariate normal case:

$$\lambda(\alpha) = \frac{\phi(\alpha)}{1 - \Phi(\alpha)}. \quad (5)$$

Its variance equivalent $\mathbb{E}[X^2|X > \alpha]$ is denoted by $\delta(\alpha)$:

$$\delta(\alpha) = \lambda(\alpha)(\lambda(\alpha) - \alpha). \quad (6)$$

Using the notation defined above, we now recall the derivation of the TKF from [15]. The first two moments of $y_k(i)$ are given by:

$$\mathbb{E}[y_k(i)|\mathbf{x}_k, \sigma_k(i)] = (1 - \Phi(\eta_k(i)))\tau_k(i) + \Phi(\eta_k(i))(C_k x_k(i) + \sigma_k(i)\lambda(-\eta_k(i))) \quad (7)$$

$$\text{Var}[y_k(i)|\mathbf{x}_k, \sigma_k(i)] = \sigma_k^2(i)[1 - \delta(\eta_k(i))], \quad (8)$$

The Kalman error $\tilde{y}_k(i)$ is then given by:

$$\tilde{y}_k(i) = y_k(i) - \mathbb{E}[y_k(i)|\mathbf{x}_{k|k-1}, \sigma_k(i)]. \quad (9)$$

Additionally, we use a diagonal $m \times m$ matrix of Bernoulli variables \mathbf{P}_k to represent the censoring of the measurements. Its elements are given by:

$$p_k(i, j) = I(y_k(i) > \tau_k(i))\delta_{i,j}, \quad (10)$$

where $\delta_{i,j}$ is the Kronecker delta function and $I(\cdot)$ is the indicator function. The expected value of the censoring variable is:

$$\mathbb{E}[p_k(i, j)] = \Phi(\eta_k(i)). \quad (11)$$

We now define the covariance matrix $\mathbf{R}_{\tilde{\mathbf{y}}\tilde{\mathbf{y}},k} = \mathbb{E}[(\mathbf{x}_k - \mathbf{x}_{k-1})\tilde{\mathbf{y}}_k^T]$:

$$\mathbf{R}_{\tilde{\mathbf{y}}\tilde{\mathbf{y}},k} = \mathbf{\Psi}_{k|k-1} \mathbf{C}_k^T \mathbb{E}[\mathbf{P}_k], \quad (12)$$

where $\mathbf{\Psi}_{k|k-1} = \mathbb{E}[(\mathbf{x}_k - \hat{\mathbf{x}}_k)(\mathbf{x}_k - \hat{\mathbf{x}}_k)^T]$ is the predicted *a priori* state error covariance. We define the column vector $\tilde{\mathbf{v}}_k$ representing the bias introduced in the measurement noise by the censoring, whose elements are $\tilde{v}_k(i) = \sigma_k(i)\lambda(-\eta_k(i))$. As in [15], we define the Kalman error covariance matrix $\mathbf{R}_{\tilde{\mathbf{y}}\tilde{\mathbf{y}},k} = \mathbb{E}[\tilde{\mathbf{y}}_k\tilde{\mathbf{y}}_k^T]$:

$$\begin{aligned} \mathbf{R}_{\tilde{\mathbf{y}}\tilde{\mathbf{y}},k} = & \mathbb{E}[\mathbf{P}_k] \mathbf{C}_k \mathbf{\Psi}_{k|k-1} \mathbf{C}_k^T \mathbb{E}[\mathbf{P}_k] + \\ & \mathbb{E}[\mathbf{P}_k(\mathbf{v}_k - \tilde{\mathbf{v}}_k)(\mathbf{v}_k - \tilde{\mathbf{v}}_k)^T \mathbf{P}_k]. \end{aligned} \quad (13)$$

The second term of the sum corresponds to the measurement covariance matrix \mathbf{V}_k , which is equal to:

$$\mathbf{V}_k = \text{diag} \begin{bmatrix} \text{Var}[y_k(1)|\hat{x}_{k|k-1}(1), \sigma_k(1)] \\ \text{Var}[y_k(2)|\hat{x}_{k|k-1}(2), \sigma_k(2)] \\ \vdots \\ \text{Var}[y_k(m)|\hat{x}_{k|k-1}(m), \sigma_k(m)] \end{bmatrix}. \quad (14)$$

The derivation in [15] assumes that \mathbf{Q}_k and \mathbf{R}_k are diagonal to simplify the notation. The derivation of the theoretical covariance matrix in the general case can be adapted from the characterization of the truncated multivariate normal in [34]. The Kalman gain is calculated as:

$$\mathbf{K}_j = \mathbf{R}_{\tilde{\mathbf{y}}\tilde{\mathbf{y}},j}^{-1} \mathbf{R}_{\tilde{\mathbf{y}}\tilde{\mathbf{y}},k}^{-1}. \quad (15)$$

The TKF is then given by:

$$\hat{\mathbf{x}}_{k|k-1} = \mathbf{A}_{k-1} \hat{\mathbf{x}}_{k-1|k-1} \quad (16)$$

$$\mathbf{\Psi}_{k|k-1} = \mathbf{A}_{k-1} \mathbf{\Psi}_{k-1|k-1} \mathbf{A}_{k-1}^T + \mathbf{Q}_{k-1} \quad (17)$$

$$\hat{\mathbf{x}}_{k|k} = \hat{\mathbf{x}}_{k|k-1} + \mathbf{R}_{\tilde{\mathbf{y}}\tilde{\mathbf{y}},k}^{-1} \mathbf{R}_{\tilde{\mathbf{y}}\tilde{\mathbf{y}},k} \tilde{\mathbf{y}}_k \quad (18)$$

$$\mathbf{\Psi}_{k|k} = (\mathbf{I}_{m \times m} - \mathbb{E}[\mathbf{P}_k]) \mathbf{R}_{\tilde{\mathbf{y}}\tilde{\mathbf{y}},k}^{-1} \mathbf{R}_{\tilde{\mathbf{y}}\tilde{\mathbf{y}},k} \mathbf{C}_k \mathbf{\Psi}_{k|k-1} \quad (19)$$

IV. A POSTERIORI NOISE COVARIANCE ESTIMATION

In this section, we derive the noise covariance estimator for the TKF. In a system with diagonal noise covariance matrices, the *a posteriori* density function of the noise covariance of a standard Kalman filter can be estimated using the Maximum

A Posteriori (MAP) coupling form [35]:

$$\hat{\mathbf{Q}}_k = \frac{1}{k} \sum_{\ell=1}^k [\hat{\mathbf{x}}_{k|\ell} - \mathbf{A}_{\ell-1} \hat{\mathbf{x}}_{k|\ell-1}] [\hat{\mathbf{x}}_{k|\ell} - \mathbf{A}_{\ell-1} \hat{\mathbf{x}}_{k|\ell-1}]^T \quad (20)$$

$$\hat{\mathbf{R}}_k = \frac{1}{k} \sum_{\ell=1}^k [y_\ell - \mathbf{C}_\ell \hat{\mathbf{x}}_{k|\ell}] [y_\ell - \mathbf{C}_\ell \hat{\mathbf{x}}_{k|\ell}]^T. \quad (21)$$

Even in the standard scenario with no censoring, the multistep terms $\hat{\mathbf{x}}_{k|\ell-1}$ and $\hat{\mathbf{x}}_{k|\ell}$ make the optimal formulation above impractical, as it cannot be described in recursive form. A practical one-step approximation is presented in [16]. In the TKF case, the derivation for the practical unbiased estimator for $\hat{\mathbf{Q}}_k$ follows from (1). The process noise covariance matrix is still $\mathbf{Q} = \mathbb{E}[(\mathbf{x}_k - \mathbf{A}_{k-1} \mathbf{x}_{k-1})(\mathbf{x}_k - \mathbf{A}_{k-1} \mathbf{x}_{k-1})^T]$, and if we assume that the ATKF state estimate is close enough to the real state, i.e., $\hat{\mathbf{x}}_{k|k} \approx \mathbf{x}_k$, an assumption that the standard TKF also requires, we get:

$$\mathbf{Q} = \mathbb{E}[(\mathbf{x}_k - \mathbf{A}_{k-1} \mathbf{x}_{k-1})(\mathbf{x}_k - \mathbf{A}_{k-1} \mathbf{x}_{k-1})^T] \quad (22)$$

$$\mathbf{Q} \approx \mathbb{E}[(\hat{\mathbf{x}}_{k|k} - \mathbf{A}_{k-1} \hat{\mathbf{x}}_{k-1|k-1})(\hat{\mathbf{x}}_{k|k} - \mathbf{A}_{k-1} \hat{\mathbf{x}}_{k-1|k-1})^T] \quad (23)$$

$$\mathbf{Q} \approx \mathbb{E}[(\hat{\mathbf{x}}_{k|k} - \hat{\mathbf{x}}_{k|k-1})(\hat{\mathbf{x}}_{k|k} - \hat{\mathbf{x}}_{k|k-1})^T] \quad (24)$$

$$\mathbf{Q} \approx \mathbb{E}[(\mathbf{K}_k \tilde{\mathbf{y}}_k)(\mathbf{K}_k \tilde{\mathbf{y}}_k)^T]. \quad (25)$$

We can now estimate the value of \mathbf{Q} from the available samples:

$$\hat{\mathbf{Q}}_k = \frac{1}{k} \sum_{j=1}^k \mathbf{K}_j \tilde{\mathbf{y}}_j \tilde{\mathbf{y}}_j^T \mathbf{K}_j^T. \quad (26)$$

The expected value of the process noise covariance is:

$$\mathbb{E}[\hat{\mathbf{Q}}_k] = \mathbb{E} \left[\frac{1}{k} \sum_{j=1}^k \mathbf{K}_j \tilde{\mathbf{y}}_j \tilde{\mathbf{y}}_j^T \mathbf{K}_j^T \right] \quad (27)$$

$$\mathbb{E}[\hat{\mathbf{Q}}_k] = \frac{1}{k} \mathbb{E} \left[\sum_{j=1}^k \mathbb{E}[\mathbf{P}_j] \mathbf{K}_j \mathbf{C}_j \mathbf{\Psi}_{j|j-1} \right] \quad (28)$$

$$\mathbb{E}[\hat{\mathbf{Q}}_k] = \mathbb{E} \left[\frac{1}{k} \sum_{j=1}^k \mathbf{\Psi}_{j|j-1} - \mathbf{\Psi}_{j|j} \right] \quad (29)$$

The derivation of (28) follows from the fact that $\mathbb{E}[\tilde{\mathbf{y}}_j \tilde{\mathbf{y}}_j^T] = \mathbf{R}_{\tilde{\mathbf{y}}\tilde{\mathbf{y}},j}$. In the following step, we use (19) to remove the Kalman gain from the equation. We can now subtract the expected value in (29) from (26) to write the unbiased estimator for the process noise covariance:

$$\hat{\mathbf{Q}}_k = \frac{1}{k} \sum_{\ell=1}^k \mathbf{K}_j \tilde{\mathbf{y}}_j \tilde{\mathbf{y}}_j^T \mathbf{K}_j^T + \mathbf{\Psi}_{j|j} - \mathbf{A} \mathbf{\Psi}_{j-1|j-1} \mathbf{A}^T. \quad (30)$$

The estimation noise covariance matrix \mathbf{R}_k does not have a linear estimator, since the Kalman error covariance matrix $\mathbf{R}_{\tilde{\mathbf{y}}\tilde{\mathbf{y}},k}$ is given by (13), which contains \mathbf{V}_k instead of \mathbf{R}_k . We get the unbiased estimator for $\hat{\mathbf{V}}_k$ by substituting the TKF equations into the one-step version of (21):

$$\hat{\mathbf{V}}_k = \frac{1}{k} \sum_{\ell=1}^k (\mathbf{I} - \mathbf{C}_j \mathbf{K}_j) (\tilde{\mathbf{y}}_j \tilde{\mathbf{y}}_j^T (\mathbf{I} - \mathbf{C}_j \mathbf{K}_j) + \mathbf{C}_j \mathbf{R}_{\tilde{\mathbf{y}}\tilde{\mathbf{y}},j}). \quad (31)$$

The derivation of (31) is the same as in [16], using the TKF modified equations instead of the standard KF. In order to estimate $\hat{\mathbf{R}}_k$, we can now simply invert (8):

$$\hat{\mathbf{R}}_k(i, i) = \frac{\hat{V}_k(i, i)}{1 - \delta(\hat{\eta}_k(i))} \quad (32)$$

$$\hat{\eta}_k(i) = \frac{C_k \hat{x}_{k|k-1}(i) - \tau_k(i)}{\hat{\sigma}_{k-1}(i)}. \quad (33)$$

The resulting heuristic estimator is not unbiased, since the function is non-linear, but corresponds to the one-step MLE for the censored Gaussian distribution, as derived by Gupta [36].

The TKF converges to the standard KF when the censoring region is far from the state value. The noise estimator also converges to the unbiased noise estimator used in the AKF. After substituting the terms in (30), the estimator is the one in [16]. The same goes for the measurement noise estimator, since $\lim_{\eta_k \rightarrow -\infty} \hat{\mathbf{R}}_k = \hat{V}_k$.

Note also that the noise estimation is computationally simple, as its only additional load with respect to the AKF is the calculation of the inverse functions in (32). Therefore, the ATKF can operate while requiring the extra computation of m normal PDFs and CDFs at each iteration.

A. Time-varying noise estimation

In order to deal with time-varying noise, the estimation of the noise covariances needs to be performed over a limited window in time. This can be done with a simple lowpass filter, so that the new estimate of the covariance is the linear combination of the old estimate and the latest sample, weighted by a factor Γ_k :

$$\Gamma_k = \frac{1 - \gamma}{1 - \gamma^k}, \quad (34)$$

where $\gamma \in [0, 1)$ is a fading factor. Lower values of the fading factor correspond to a higher weight to new samples, and setting $\gamma = 0$ is equivalent to only considering the latest sample. However, the covariance samples are sensitive to noise outliers, and the estimator might even diverge. For this reason, the estimator can use an Innovation Covariance Estimator (ICE) that averages the covariance samples over a rectangular sliding window to guarantee that noise covariance matrices are semidefinite positive [37]:

$$\xi_k = \frac{1}{N} \sum_{j=k-N+1}^k [\tilde{\mathbf{y}}_j \tilde{\mathbf{y}}_j^T], \quad (35)$$

where N is the size of the sliding window. The ICE is another lowpass filter, and its length determines the reactivity of the estimator. If the noise statistics are fast-varying, shorter windows are recommended. It is now possible to rewrite the estimator recursive equations, considering (34) and (35):

$$\hat{\mathbf{Q}}_k = (1 - \Gamma_k) \hat{\mathbf{Q}}_{k-1} + \Gamma_k \left(\mathbf{K}_k \xi_k \mathbf{K}_k^T + \Psi_{k|k} - \mathbf{A}_k \Psi_{k-1|k-1} \mathbf{A}_k^T \right) \quad (36)$$

$$\hat{V}_k = (\mathbf{I} - \mathbf{C}_k \mathbf{K}_k) (\mathbf{K}_k \xi_k (\mathbf{I} - \mathbf{C}_k \mathbf{K}_k) + \mathbf{C}_k \mathbf{R}_{\tilde{\mathbf{y}}, k}) \quad (37)$$

$$\hat{\mathbf{R}}_k = (1 - \Gamma_k) \hat{\mathbf{R}}_{k-1} + \Gamma_k (\mathbf{I} - \text{diag}(\delta(\hat{\eta}_k)))^{-1} \hat{V}_k \quad (38)$$

The full ATKF is given by the full estimator in (36)-(38), along with the update formulas in (16)-(19).

V. PERFORMANCE EVALUATION

In this section, we present the results from two simulations, whose parameters are taken from [15] and [38]. The first scenario is simple and shows the limits of the Kalman approach in censored scenarios, and how the Tobit version of the filter can overcome them. In the second, a positioning application is extended to include the censored case, in which the position information is not available outside a limited region. We also included the original two-dimensional scenario from [15] in Appendix A to provide a more complete comparison, even though it is not related to IoT scenarios. The ATKF will be compared with three other filters: the standard KF and the TKF with the correct values of \mathbf{Q}_k and \mathbf{R}_k , and the AKF from [16]. In this way, we will show that the ATKF achieves almost the same performance as the TKF while estimating the noise covariances online. We set $\gamma = 0.33$ and $N = 30$ in both examples.

A. Constant value estimation

In the first example, we will estimate a 1D constant value below the censoring limit. In this case, we have $x = -1$, $Q = 0$, $R = 1$, and $\tau = 0$. This means that any negative measurement value will be censored, and the state is one standard deviation below the limit. As Fig. 1 shows, most of the samples are censored. The initial conditions for the filters are $\hat{x}_0 = 5$ and $\hat{\Psi}_0 = 25$, and the two adaptive filters are initialized with $\hat{Q}_0 = 1$ and $\hat{R}_0 = 1$. Fig. 1 shows that the KF and AKF have a similar performance, staying above the censoring limit and having a significant error, while the TKF estimates the state correctly after relatively few steps. The ATKF has a noisier evolution for the first 50 steps, but quickly converges to the true value of x .

Fig. 2 shows the evolution of the squared error for the different filters. The error is larger than 1 for the KF and AKF, whose estimates are always above the censoring threshold, while the error of the TKF and ATKF soon reaches very small values. In this case, the ATKF even performs slightly better than the TKF after the initial phase, with a lower Mean Squared Error (MSE), but both errors are negligible.

B. VLC positioning

A classic IoT application is indoor positioning: mobile robots and simple sensor nodes can combine their own internal sensors and the parameters of a wireless signal received from a known base station through sensor fusion, using the RSS [39] or Angle of Arrival (AoA) [40] to improve their localization accuracy. Over the past few years, VLC measurements have become a viable alternative to classic WiFi or BLE-based positioning methods [41], and Kalman filters have already been used to improve tracking in this kind of application [42].

The third example we show uses VLC to estimate a mobile robot's position and an internal gyroscope to measure its heading. The dynamic system we use is the same as in [43],

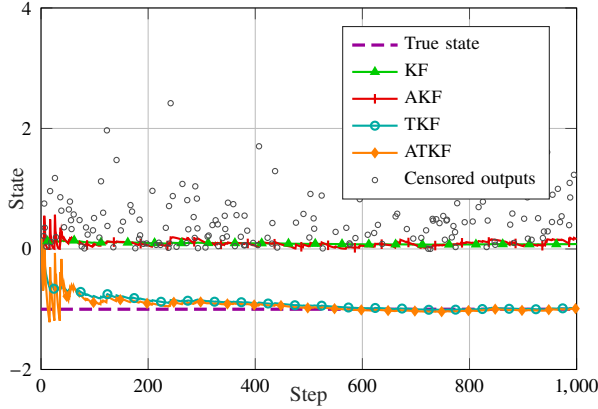


Figure 1: 1D example: estimation of a constant value one standard deviation of the measurement noise below the censoring limit.

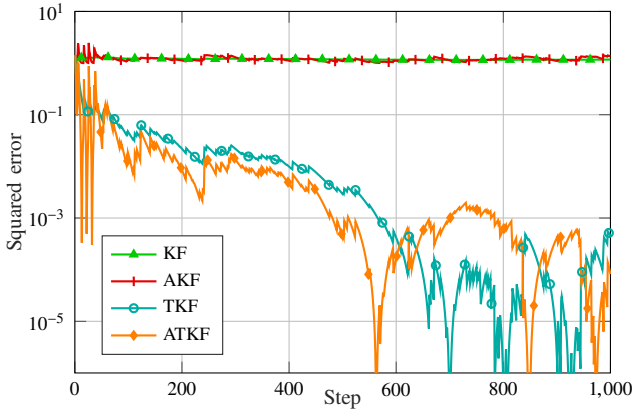


Figure 2: 1D example: squared error of the filters.

with the same parameters, which are reported in Table I. We consider a timestep T , and the state \mathbf{x}_k of the robot at step k is denoted by its position $(x_{k,1}, x_{k,2})$ and its heading θ_k . We assume that it has two independent wheels, with a radius R_w and placed at a distance d_w . The robot can maintain a speed v , and its turning rate is $\Delta\theta$. The motion update equation is given by:

$$\begin{bmatrix} x_{k+1,1} \\ x_{k+1,2} \\ \theta_{k+1} \end{bmatrix} = \begin{bmatrix} x_{k,1} \\ x_{k,2} \\ \theta_k \end{bmatrix} + \begin{bmatrix} vT \cos\left(\theta_k + \frac{\Delta\theta}{2}\right) \\ vT \sin\left(\theta_k + \frac{\Delta\theta}{2}\right) \\ \Delta\theta_k \end{bmatrix} + \mathbf{w}_k, \quad (39)$$

where $\mathbf{w}_k \sim \mathcal{N}(0, \mathbf{Q})$ is the Gaussian process noise. The Kalman update matrix \mathbf{A}_{k+1} is the Jacobian matrix of the update function, containing its partial derivatives to the state \mathbf{x}_k :

$$\mathbf{A}_{k+1} = \begin{bmatrix} 1 & 0 & -vT \sin\left(\theta_k + \frac{\Delta\theta}{2}\right) \\ 0 & 1 & vT \cos\left(\theta_k + \frac{\Delta\theta}{2}\right) \\ 0 & 0 & 1 \end{bmatrix}. \quad (40)$$

The measurement matrix $\mathbf{C} = \mathbf{I}_{3 \times 3}$ gives the following mea-

surement function:

$$\mathbf{y}_k = \mathbf{x}_k + \mathbf{v}_k, \quad (41)$$

where $\mathbf{v}_k \sim \mathcal{N}(0, \mathbf{R})$ is the Gaussian measurement noise.

We can now define the covariance matrices of the two noise components:

$$\mathbf{Q}_k = vT k_w \mathbf{W} \mathbf{W}^T, \quad (42)$$

where \mathbf{W}_k is the Jacobian matrix of the update function given in (39) with respect to \mathbf{w}_k :

$$W_{k,i,j} = \frac{\partial x_{k,i}}{\partial w_{k,j}}. \quad (43)$$

In this case, \mathbf{Q}_k is not symmetrical, so the ATKF will have an additional source of errors. The measurement noise covariance matrix \mathbf{R}_k is defined as:

$$\mathbf{R}_k = \begin{bmatrix} \sigma_{\text{VLC}}^2 & 0 & 0 \\ 0 & \sigma_{\text{VLC}}^2 & 0 \\ 0 & 0 & \sigma_{\text{gyro}}^2 \end{bmatrix}, \quad (44)$$

where σ_{VLC}^2 is the VLC positioning error variance and σ_{gyro}^2 is the gyroscopic attitude measurement error variance.

In our system, we consider a single VLC transmitter, whose signal can only be sensed underneath a roof cover: if the robot moves outside the covered area, sunlight will interfere with the VLC system [44]. making the localization measurement unusable. The roof is considered as a square of 1 m, and the VLC transmitter is placed at one of its vertices. The effect of the interference is shown in Fig. 3: measurements are only available in the shaded area, and the values outside are censored. The plot clearly shows that the TKF and ATKF are able to follow the robot's path, while the standard filters Even if the TKF and ATKF seem to follow the trajectory correctly, Fig. 4 shows that the ATKF's timing is off, resulting in a 0.5 m offset in its position estimate while the TKF remains very precise. However, the performance of the filter is still very good considering the extremely limited amount of information available to it.

VI. CONCLUSION

This work presents a recursive noise covariance estimation method for the TKF, showing a small performance loss with respect to the TKF with full *a priori* knowledge. The ATKF is inspired by the approach from [16], it does not add significant computational complexity to a standard TKF, and it also

Table I: VLC positioning parameters.

Parameter	Value	Description
R_w	5 cm	Robot wheel radius
d_w	30 cm	Robot wheel distance
T	0.05 s	Filter timestep
k_w	0.0003	Wheel-floor interaction parameter
σ_{VLC}	0.06 cm	VLC positioning error
σ_{gyro}	3°	Gyroscopic attitude measurement error
θ_0	45°	Initial heading
$\Delta\theta$	0°/s	Robot turning rate
v	1 m/s	Robot speed

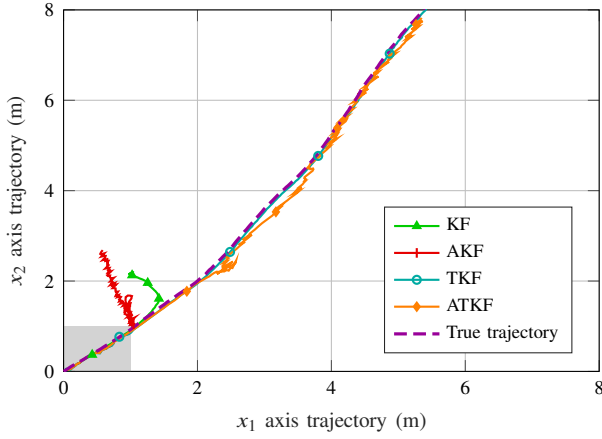


Figure 3: VLC positioning: estimated trajectories.

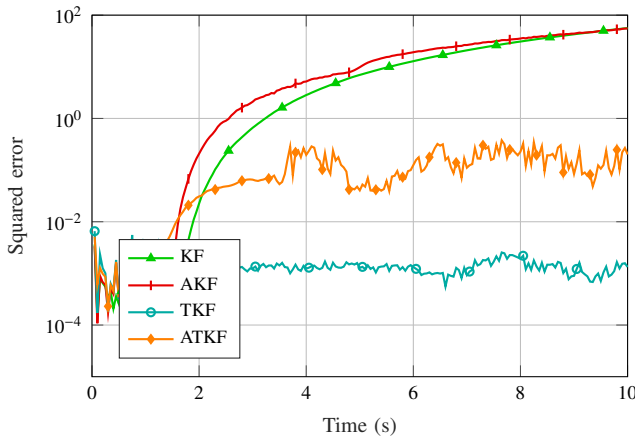


Figure 4: VLC positioning: squared error of the filters.

converges to the standard AKF when the state is far from the censoring region. The estimate of the measurement noise is biased because of the non-linearity of the relation between innovation variance and measurement noise variance, but it is optimal if we consider a one-step memory. The estimation method is also robust to time-varying noise statistics and censoring thresholds. The ATKF is tested in a simple example and an IoT positioning application, and shown to be a versatile and powerful tool to improve the estimation and tracking of variables with censored sensor data, which often occur in this networking paradigm.

Future work on the subject includes the adaptation to the Tobit Type I model of other AKF methods such as ALS, which might outperform the recursive approach in some scenarios. The implementation of the ATKF in actual IoT devices is also an interesting subject of research. Finally, the extension to non-diagonal noise covariance matrices will be considered in an extension of this work.

APPENDIX

In this appendix, we provide another comparison with the TKF, using the scenario from the original work [15], which models ballistic roll using censored magnetometer measurements [45]. This kind of system is often used in Unmanned

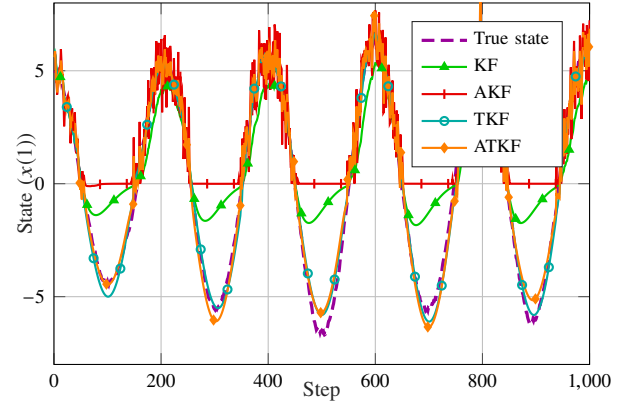


Figure 5: Attitude estimation: estimation of the observed state component.

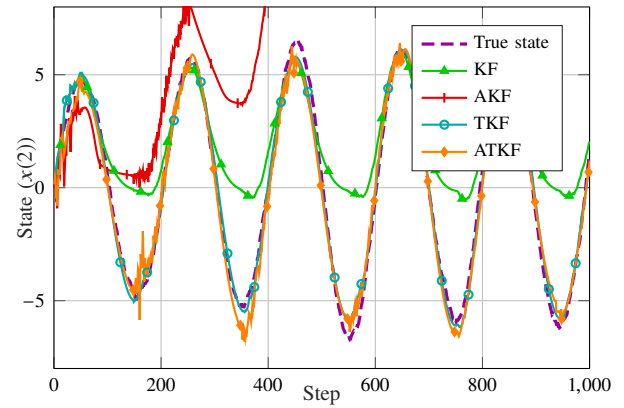


Figure 6: Attitude estimation: estimation of the hidden state component.

Aerial Vehicles (UAVs) to estimate the attitude [38], and Kalman-based tracking has already been proposed in the literature [46]. The dynamic system in this example can be easily adapted to a fixed-wing UAV performing banking maneuvers [47], and even to a ground vehicle making sharp turns [48]. The measurement is one-dimensional ($m = 1$), and it is derived from a 2D hidden state ($n = 2$). In this case, we need to use an EKF, as the equations of the system are nonlinear.

$$\mathbf{A}_k = \alpha \begin{bmatrix} \cos(\omega) & -\sin(\omega) \\ \sin(\omega) & \cos(\omega) \end{bmatrix} \quad (45)$$

$$\mathbf{C}_k = \begin{bmatrix} 1 & 0 \end{bmatrix} \quad (46)$$

The oscillator frequency is $\omega = 0.005 \cdot 2\pi$ and the gain is $\alpha = 1$, with a sampling period $T = 1$. The censoring threshold is still $\tau = 0$. In this case, we set $\mathbf{Q}_k = \mathbf{I} \cdot 0.0025$ and $\sigma_k^2 = 1$. The presence of a low process noise makes the system more irregular, and thus harder to estimate correctly when the measurements are censored. The initial conditions of the filters are $\hat{\mathbf{x}}_0 = [5 \ 0]^T$ and $\Psi_0 = \mathbf{I}$. As in the previous example, the adaptive filters are initialized with $\hat{\mathbf{Q}}_0 = \mathbf{I}$ and $\hat{R}_0 = 1$.

Fig. 5 shows the evolution of the first state variable. When the measurements are not censored, the KF is the only one that does not correctly follow the trend of the hidden state,

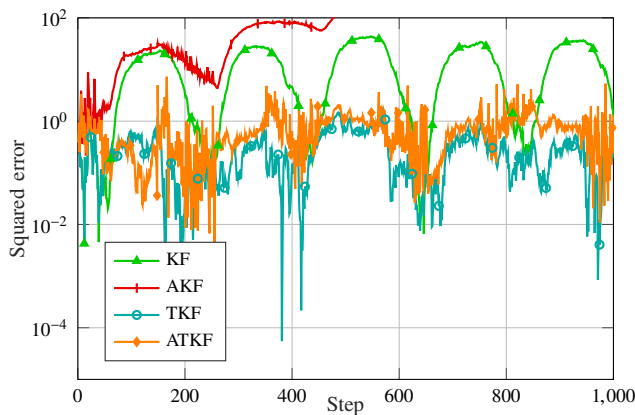


Figure 7: Attitude estimation: squared error of the filters.

even if the AKF is noisier than either the TKF or the ATKF. However, the AKF never goes below 0 in its estimate, while the KF manages to follow the state in its valleys, even as it strongly underestimates their magnitude. The TKF and ATKF also make an error on the valley amplitude, probably because of the process noise, but the error is far lower. Fig. 6 shows the evolution of the second state variable, which is not observed directly. In this case, the AKF quickly diverges, as it is unable to get a correct estimate of the noise covariances. The KF does better, underestimating the valleys but correctly estimating the peaks. On the other hand, the TKF and ATKF only make small mistakes on the amplitudes of the minima and maxima, correctly following the trend even when the measurement of the first state variable is censored and the second one is hidden.

Fig. 7 shows the evolution of the squared error in this example: in this case, the ATKF does slightly worse than the TKF, with a MSE of 0.75, while the TKF has 0.34. However, the error of the two filters is still lower than the measurement noise variance, even when the noise is censored. At the same time, the divergence of the AKF and the underestimation of the censored lobes by the standard KF make them have a far higher error.

REFERENCES

- [1] J. Gubbi, R. Buyya, S. Marusic, and M. Palaniswami, "Internet of Things (IoT): A vision, architectural elements, and future directions," *Future Generation Computer Systems*, vol. 29, no. 7, pp. 1645–1660, Sep. 2013.
- [2] L. Zhang, J. Liu, and H. Jiang, "Energy-efficient location tracking with smartphones for IoT," in *Sensors*. IEEE, Oct. 2012, pp. 1–4.
- [3] S. Gite and H. Agrawal, "On context awareness for multisensor data fusion in IoT," in *2nd International Conference on Computer and Communication Technologies*. Springer, Jul. 2016, pp. 85–93.
- [4] D. Kumar, S. Rajasegarar, and M. Palaniswami, "Automatic sensor drift detection and correction using Spatial Kriging and Kalman filtering," in *International Conference on Distributed Computing in Sensor Systems*. IEEE, May 2013, pp. 183–190.
- [5] D. Macagnano, G. Destino, and G. Abreu, "Indoor positioning: A key enabling technology for IoT applications," in *World Forum on Internet of Things (WF-IoT)*. IEEE, Mar. 2014, pp. 117–118.
- [6] A. J. Jara, P. Lopez, D. Fernandez, J. F. Castillo, M. A. Zamora, and A. F. Skarmeta, "Mobile digcovery: discovering and interacting with the world through the Internet of Things," *Personal and Ubiquitous Computing*, vol. 18, no. 2, pp. 323–338, Feb. 2014.
- [7] C. Perera, D. S. Talagala, C. H. Liu, and J. C. Estrella, "Energy-efficient location and activity-aware on-demand mobile distributed sensing platform for sensing as a service in IoT clouds," *IEEE Transactions on Computational Social Systems*, vol. 2, no. 4, pp. 171–181, Dec. 2015.
- [8] K. Lin, M. Chen, J. Deng, M. M. Hassan, and G. Fortino, "Enhanced fingerprinting and trajectory prediction for IoT localization in smart buildings," *IEEE Transactions on Automation and Engineering*, vol. 13, no. 3, pp. 1294–1307, Apr. 2016.
- [9] N. Bui, M. Cesana, S. A. Hosseini, Q. Liao, I. Malanchini, and J. Widmer, "A survey of anticipatory mobile networking: Context-based classification, prediction methodologies, and optimization techniques," *IEEE Communications Surveys & Tutorials*, vol. 19, no. 3, pp. 1790–1821, Apr. 2017.
- [10] R. E. Kalman, "A new approach to linear filtering and prediction problems," *Journal of Basic Engineering*, vol. 82, no. 1, pp. 35–45, Mar. 1960.
- [11] N. Yu, X. Zhan, S. Zhao, Y. Wu, and R. Feng, "A precise dead reckoning algorithm based on Bluetooth and multiple sensors," *IEEE Internet of Things Journal*, vol. 5, no. 1, pp. 336–351, 2017.
- [12] S.-K. Weng, C.-M. Kuo, and S.-K. Tu, "Video object tracking using adaptive Kalman filter," *Journal of Visual Communication and Image Representation*, vol. 17, no. 6, pp. 1190–1208, Dec. 2006.
- [13] F. Dellaert and C. Thorpe, "Robust car tracking using Kalman filtering and Bayesian templates," in *Conference on Intelligent Transportation Systems (ITSC)*, vol. 1. IEEE, Oct. 1997, pp. 72–83.
- [14] J. Tobin, "Estimation of relationships for limited dependent variables," *Econometrica: Journal of the Econometric Society*, vol. 26, no. 1, pp. 24–36, Jan. 1958.
- [15] B. Allik, C. Miller, M. J. Piovoso, and R. Zurakowski, "The Tobit Kalman filter: an estimator for censored measurements," *IEEE Transactions on Control Systems Technology*, vol. 24, no. 1, pp. 365–371, Jun. 2015.
- [16] W. Gao, J. Li, G. Zhou, and Q. Li, "Adaptive Kalman filtering with recursive noise estimator for integrated SINS/DVL systems," *The Journal of Navigation*, vol. 68, no. 1, pp. 142–161, Jan. 2015.
- [17] M. M. Rana and L. Li, "Kalman filter based microgrid state estimation using the Internet of Things communication network," in *12th International Conference on Information Technology-New Generations*. IEEE, Apr. 2015, pp. 501–505.
- [18] T. D. Nguyen, J. Y. Khan, and D. T. Ngo, "An effective energy-harvesting-aware routing algorithm for WSN-based IoT applications," in *International Conference on Communications (ICC)*. IEEE, May 2017, pp. 1–6.
- [19] Y.-s. Gong and Y. Zhang, "Research of short-term traffic volume prediction based on Kalman filtering," in *6th International Conference on Intelligent Networks and Intelligent Systems (ICINIS)*. IEEE, Nov. 2013, pp. 99–102.
- [20] Y.-X. Zhao, Y.-S. Su, and Y.-C. Chang, "A real-time bicycle record system of ground conditions based on Internet of Things," *IEEE Access*, vol. 5, pp. 17 525–17 533, Aug. 2017.
- [21] Y. Huang, W. Yu, E. Ding, and A. Garcia-Ortiz, "EpKF: Energy efficient communication schemes based on kalman filter for iot," *IEEE Internet of Things Journal*, Feb. 2019.
- [22] A. Ozer and E. John, "Improving the accuracy of Bluetooth Low Energy indoor positioning system using Kalman filtering," in *International Conference on Computational Science and Computational Intelligence (CSCI)*. IEEE, Dec. 2016, pp. 180–185.
- [23] W. Bakkali, M. Kieffer, M. Lalam, and T. Lestable, "Kalman filter-based localization for Internet of Things LoRaWAN end points," in *28th Annual International Symposium on Personal, Indoor, and Mobile Radio Communications (PIMRC)*. IEEE, Oct. 2017, pp. 1–6.
- [24] Y. Zhuang, Q. Wang, M. Shi, P. Cao, L. Qi, and J. Yang, "Low-power centimeter-level localization for indoor mobile robots based on Ensemble Kalman smoother using Received Signal Strength," *IEEE Internet of Things Journal*, 2019.
- [25] B. Sinopoli, L. Schenato, M. Franceschetti, K. Poolla, M. I. Jordan, and S. S. Sastry, "Kalman filtering with intermittent observations," *IEEE Transactions on Automatic Control*, vol. 49, no. 9, pp. 1453–1464, Sep. 2004.
- [26] B. Allik, C. Miller, M. J. Piovoso, and R. Zurakowski, "Nonlinear estimators for censored data: a comparison of the EKF, the UKF and the Tobit Kalman filter," in *American Control Conference (ACC)*. IEEE, Jul. 2015, pp. 5146–5151.
- [27] B. Allik, "Particle filter for target localization and tracking leveraging lack of measurement," in *American Control Conference (ACC)*. IEEE, May 2017, pp. 1592–1597.
- [28] K. Loumponias, A. Dimou, N. Vretos, and P. Daras, "Adaptive Tobit Kalman-based tracking," in *14th International Conference on Signal-Image Technology & Internet-Based Systems (SITIS)*. IEEE, Jun. 2018, pp. 70–76.

- [29] R. Mehra, "On the identification of variances and adaptive kalman filtering," *IEEE Transactions on Automatic Control*, vol. 15, no. 2, pp. 175–184, Apr. 1970.
- [30] M. R. Rajamani and J. B. Rawlings, "Estimation of the disturbance structure from data using semidefinite programming and optimal weighting," *Automatica*, vol. 45, no. 1, pp. 142–148, Jan. 2009.
- [31] L. Zanni, J.-Y. Le Boudec, R. Cherkaoui, and M. Paolone, "A prediction-error covariance estimator for adaptive kalman filtering in step-varying processes: application to power-system state estimation," *IEEE Transactions on Control Systems Technology*, vol. 25, no. 5, pp. 1683–1697, Dec. 2016.
- [32] H. Geng, Z. Wang, Y. Cheng, F. E. Alsaadi, and A. M. Dobaie, "State estimation under non-Gaussian Lévy and time-correlated additive sensor noises: A modified Tobit Kalman filtering approach," *Signal Processing*, vol. 154, pp. 120–128, Jan. 2019.
- [33] F. Han, H. Dong, Z. Wang, G. Li, and F. E. Alsaadi, "Improved Tobit Kalman filtering for systems with random parameters via conditional expectation," *Signal Processing*, vol. 147, pp. 35–45, Jun. 2018.
- [34] S. Rosenbaum, "Moments of a truncated bivariate normal distribution," *Journal of the Royal Statistical Society: Series B (Methodological)*, vol. 23, no. 2, pp. 405–408, Jul. 1961.
- [35] A. P. Sage and G. W. Husa, "Adaptive filtering with unknown prior statistics," in *Joint Automatic Control Conference*, no. 7, Aug. 1969, pp. 760–769.
- [36] A. Gupta, "Estimation of the mean and standard deviation of a normal population from a censored sample," *Biometrika*, vol. 39, no. 3/4, pp. 260–273, Dec. 1952.
- [37] D.-J. Jwo and T.-P. Weng, "An adaptive sensor fusion method with applications in integrated navigation," *The Journal of Navigation*, vol. 61, no. 4, pp. 705–721, Oct. 2008.
- [38] Y.-P. Huang, L. Sithole, and T.-T. Lee, "Structure from motion technique for scene detection using autonomous drone navigation," *IEEE Transactions On Systems, Man, And Cybernetics: Systems*, Sep. 2017.
- [39] A. Zanella, "Best practice in RSS measurements and ranging," *IEEE Communications Surveys & Tutorials*, vol. 18, no. 4, pp. 2662–2686, Apr. 2016.
- [40] D. Niculescu, "Positioning in ad hoc sensor networks," *IEEE Network*, vol. 18, no. 4, pp. 24–29, Jul. 2004.
- [41] M. Rahaim, G. B. Prince, and T. D. Little, "State estimation and motion tracking for spatially diverse VLC networks," in *Global Communication Conference (GLOBECOM) Workshops*. IEEE, Dec. 2012, pp. 1249–1253.
- [42] Z. Vatansever and M. Brandt-Pearce, "Visible light positioning with diffusing lamps using an extended Kalman filter," in *Wireless Communications and Networking Conference (WCNC)*. IEEE, Mar. 2017, pp. 1–6.
- [43] N.-T. Nguyen, N.-H. Nguyen, V.-H. Nguyen, K. Sripimanwat, and A. Suebsomran, "Improvement of the VLC localization method using the Extended Kalman Filter," in *IEEE Region 10 Conference (TENCON)*. IEEE, Oct. 2014, pp. 1–6.
- [44] S. M. Nlom, K. Ouahada, A. R. Ndjiongue, and H. C. Ferreira, "Evaluation of the SFSK-OOK integrated PLC-VLC system under the influence of sunlight," in *International Symposium on Networks, Computers and Communications (ISNCC)*. IEEE, May 2017, pp. 1–5.
- [45] B. Allik, M. Ilg, and R. Zurkowski, "Ballistic roll estimation using EKF frequency tracking and adaptive noise cancellation," *IEEE Transactions on Aerospace and Electronic Systems*, vol. 49, no. 4, pp. 2546–2553, Oct. 2013.
- [46] H. G. De Marina, F. J. Pereda, J. M. Giron-Sierra, and F. Espinosa, "UAV attitude estimation using unscented Kalman filter and TRIAD," *IEEE Transactions on Industrial Electronics*, vol. 59, no. 11, pp. 4465–4474, Aug. 2011.
- [47] M. Euston, P. Coote, R. Mahony, J. Kim, and T. Hamel, "A complementary filter for attitude estimation of a fixed-wing UAV," in *2008 IEEE/RSJ International Conference on Intelligent Robots and Systems*. IEEE, Sep. 2008, pp. 340–345.
- [48] J. Garcia Guzman, L. Prieto Gonzalez, J. Pajares Redondo, S. Sanz Sanchez, and B. Boada, "Design of low-cost vehicle roll angle estimator based on Kalman filters and an IoT architecture," *Sensors*, vol. 18, no. 6, p. 1800, Jun. 2018.